

Neutron drops radii probed by the neutron skin thickness of nuclei

P. W. Zhao¹ and S. Gandolfi²

¹*Physics Division, Argonne National Laboratory, Argonne, Illinois 60439, USA*

²*Theoretical Division, Los Alamos National Laboratory,
Los Alamos, New Mexico 87545, USA*

Abstract

Multi-neutron systems are crucial to understand the physics of neutron-rich nuclei and neutron stars. Neutron drops, neutrons confined in an external field, are investigated systematically in both non-relativistic and relativistic density functional theories and with *ab initio* calculations. We demonstrate a strong linear correlation, which is universal in the realm of mean-field models, between the root-mean-square (rms) radii of neutron drops and the neutron skin thickness of ²⁰⁸Pb and ⁴⁸Ca; i.e., the difference between the neutron and proton rms radii of a nucleus. Due to its high quality, this correlation can be used to deduce the radii of neutron drops from the measured neutron skin thickness in a model-independent way, and the radii obtained for neutron drops can provide a useful constraint for realistic three neutron forces. This correlation, together with high-precision measurements of the neutron skin thicknesses of ²⁰⁸Pb and ⁴⁸Ca, will have an enduring impact on the understanding of multi-neutron interactions, neutron-rich nuclei, neutron stars, etc.

PACS numbers: 21.60.Jz, 21.10.Gv, 21.30.-x, 21.45.Ff

Pure neutron systems have attracted considerable attention in nuclear physics, since their properties are crucial for understanding neutron-rich systems ranging from microscopic rare isotopes at the femtometer scale to macroscopic neutron stars. On the one hand, they are very useful to probe possible new physics for nuclei with large isospin in as yet unexplored regions of the nuclear chart [1]. Such interests are supported further by the advent of new rare-isotope facilities [2] and also by the quest to understand the origin of the elements in the Universe through nucleosynthesis processes [3, 4]. On the other hand, understanding the inner crust of neutron stars also requires accurate knowledge of inhomogeneous neutron matter [5–7].

Although a candidate resonant tetraneutron state was proposed recently [8], most multi-neutron systems are not self-bound and, thus, an external potential must be employed to produce bound states; i.e., the so-called “neutron drops”. Due to its simplicity, a neutron drop can serve as a unique test case for various nuclear many-body methods; e.g., *ab initio* approaches for light nuclei and density functional theories (DFTs) for heavy ones. The former solve directly a many-body Hamiltonian with realistic nucleon-nucleon (NN) and three-nucleon (3N) interactions, while the latter resort to a variation of an approximated energy functional with respect to nucleon densities. Moreover, neutron drops also provide an essential test for density matrix expansion (DME) techniques, which aim to build DFTs from realistic NN and 3N interactions [9], and can describe properties of neutron-rich nuclei [10, 11].

So far, neutron drops have been studied with many *ab initio* approaches. Quantum Monte Carlo (QMC) [12] studies for neutron drops can be traced back to the 1990s, and only light droplets with $N = 6, 7, 8$ were calculated at that time [13]. Systematic calculations, covering a wide range of neutron numbers and external potentials, have been performed recently with high-accuracy phenomenological and chiral NN+3N interactions [14–17]. These *ab initio* solutions for neutron drops provide important references for nuclear energy density functionals which are usually determined by fitting to available nuclei. In comparison with the QMC calculations, traditional Skyrme density functionals considerably overbind neutron drops and yield too-large a spin-orbit splitting [13, 14].

All density-functional studies of neutron drops hitherto are in the framework of non-relativistic DFTs, and a relativistic study is still missing. Relativistic (covariant) DFTs, which invoke a different organization of the nuclear many-body problem, are particularly

compelling because the spin degrees of freedom dictated by relativity can be naturally included [18, 19]. On the other hand, the existing predictions vary largely among different theories, since neither the isospin $T = 3/2$ component of the 3N force [20, 21] nor the isovector parts (neutrons and protons contribute with opposite sign) of the density functionals [22] are clearly known.

Since it is not possible to carry out direct measurements, a connection between the neutron drop and an isospin-sensitive observable in finite nuclei can be of help to understand the properties of neutron drops further. The neutron skin thickness; i.e., the difference between neutron and proton root-mean-square (rms) radii $\Delta r_{np} = r_n - r_p$, is a typical isospin-sensitive observable for finite nuclei. Its connection to the symmetry energy of nuclear matter has attracted a lot of attention [23–26]. Moreover, worldwide efforts have been made to measure Δr_{np} through parity-violating electron scattering [27], coherent pion photoproduction [28], elastic proton scattering [29], antiprotonic atoms [30, 31], electric dipole polarizability [32, 33], and other methods. In particular, by measuring parity-violation in electron scattering, the lead and calcium radius experiments, PREX and CREX, at JLab aim to provide a Δr_{np} value for ^{208}Pb and ^{48}Ca independent of most strong interaction uncertainties [34].

In this Letter, we focus on the connection between the observable Δr_{np} and neutron drops. To this end, a systematic investigation of neutron drops has been carried out with both non-relativistic [35] and relativistic DFTs [36]. Many well-determined density functionals, widely used for nuclear and astrophysical problems, have been employed in the calculations. By doing so, a strong linear correlation between the neutron skin thickness Δr_{np} and the rms radii R of neutron drops is revealed. This correlation is universal with respect to the variation in neutron number and the strength of an external field for neutron drops, once the central density of the drop is close to nuclear saturation density. This allows one to extract R of neutron drops from the measured neutron skin thickness in a model-independent way.

The skin thickness of large nuclei is correlated to the slope L of the symmetry energy, which is directly related to the Equation of State (EOS) of pure neutron matter and to the radii of neutron stars [37–39]. In particular, a strong linear correlation between the skin thickness of ^{208}Pb and the value of L has been demonstrated within mean-field models [40]. In this Letter, we will also discuss the relation between radii of neutron drops and the value of L from the EOS in the framework of both mean-field models and *ab initio* calculations

with several microscopic Hamiltonians. We employ the auxiliary field diffusion Monte Carlo (AFDMC) method [41] to calculate the energy and radii of 20 neutrons in a harmonic oscillator trap [14] and the EOS of neutron matter [42] using several nuclear Hamiltonians, including the Argonne AV8' and AV8'+UIX [43], and local chiral forces at next-to-next-to-leading-order (N²LO) [44, 45].

We first present the first relativistic study of neutron drops in the framework of covariant DFT. The approach starts from a Lagrangian and the corresponding Kohn-Sham equations have the form of a Dirac equation with effective fields $S(\mathbf{r})$ and $V(\mathbf{r})$ derived from this Lagrangian [46]. For neutron drops, these fields are assumed to be spherical and the calculations are carried out with an external field V_{ex} which, in this work, has the form of a harmonic oscillator (HO) field,

$$[\boldsymbol{\alpha} \cdot \mathbf{p} + \beta(m + S) + V + V_{ex}]\psi_k = \epsilon_k \psi_k. \quad (1)$$

Here $V_{ex} = (m\omega^2/2)r^2$ is the external HO field with $\hbar^2/m = 41.44$ MeV fm². The fields S and V are connected in a self-consistent way to densities, so this equation requires an iterative solution, which yields the total energies, rms radii, etc. The pairing correlations are considered by solving the full relativistic Hartree-Bogoliubov (RHB) problem with a separable pairing force [47]. For details, see Refs. [46, 48, 49].

The calculations were carried out with six typical relativistic density functionals shown to be successful in many applications for finite nuclei. They cover nearly all the existing ways to build a relativistic functional; i.e., the nonlinear meson exchange functionals NL3 [50] and PK1 [51], density-dependent meson exchange ones DD-ME2 [52] and PKDD [51], a nonlinear point coupling one PC-PK1 [53], as well as the density-dependent point coupling one DD-PC1 [54]. In Fig. 1, the calculated total energies for neutron drops are presented by scaling with the Thomas-Fermi N -dependence ($N^{4/3}$) and the HO strength ($\hbar\omega = 10$ MeV). For comparison, the *ab initio* QMC results obtained in Refs. [14, 15], are also given, where the AV8' NN interaction [43] is used with two different 3N interactions, Urbana IX (UIX) [43] and Illinois-7 (IL7) [55].

The 3N force IL7 is known to be far too attractive at high densities in pure neutron systems [15, 56], and it conflicts with the observations in two-solar-mass neutron stars. Thus, as indicated in Fig. 1, the significant reduction of energies given by adding IL7 to AV8' for the droplets with large neutron numbers should not be viewed as reliable. All the

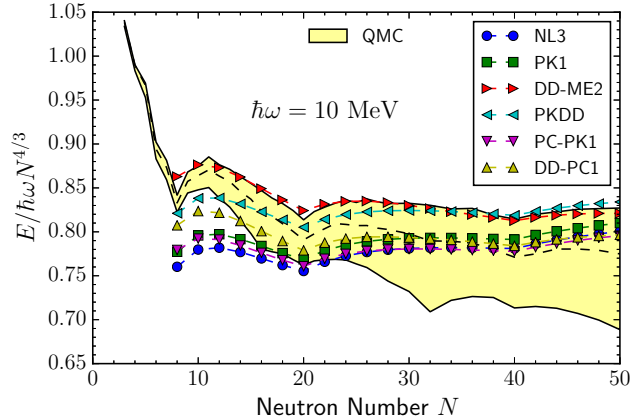


FIG. 1. (color online) Total energies (scaled by $\hbar\omega N^{4/3}$) of N -neutron systems in an harmonic oscillator (HO) trap ($\hbar\omega = 10$ MeV) predicted with various relativistic density functionals (solid symbols). The shaded area indicates the *ab initio* QMC results from Refs. [14, 15] for the NN interaction AV8' (center dashed line) as well as the AV8' plus 3N interactions of UIX (upper solid line) and IL7 (lower solid line).

density-functional results here are larger than those given solely by the AV8' Hamiltonian at large neutron numbers. This is also consistent with the results given by adding the UIX interaction to AV8', in particular, for the PKDD and DD-ME2 functionals. Although other functionals provide slightly lower energies, it should be noted that the recent *ab initio* study with chiral Hamiltonians indicates only weak contributions from the inclusion of the chiral 3N forces [16].

For light nuclei (up to $A=12$), however, IL7 provides a much better description than either AV8' or AV8'+UIX, which typically underbind these nuclei [12]. This suggests that the IL7 force may be more reliable for the droplets with small neutron numbers. Moreover, Ref. [15] demonstrates that the AV8'+IL7 results below 12 neutrons are, indeed, very similar to the NCSM ones with a nonlocal NN interaction JISP16 [57], which also gives a good description of light nuclei. The density-functional results in Fig. 1, except those for the DD-ME2 functional, are also closer to AV8'+IL7 at small neutron numbers, in particular those computed with the PKDD and DD-PC1 functionals. Fig. 1 also shows that the uncertainties associated with the realistic 3N forces and the isovector parts of the density functionals are almost at the same level when predicting neutron drop properties. Therefore, an experimental knowledge can be very helpful to probe both. However, since it is hardly

possible to directly measure a neutron drop, we intend here to connect its properties to an isospin-sensitive observable of finite nuclei; e.g., the neutron skin thickness.

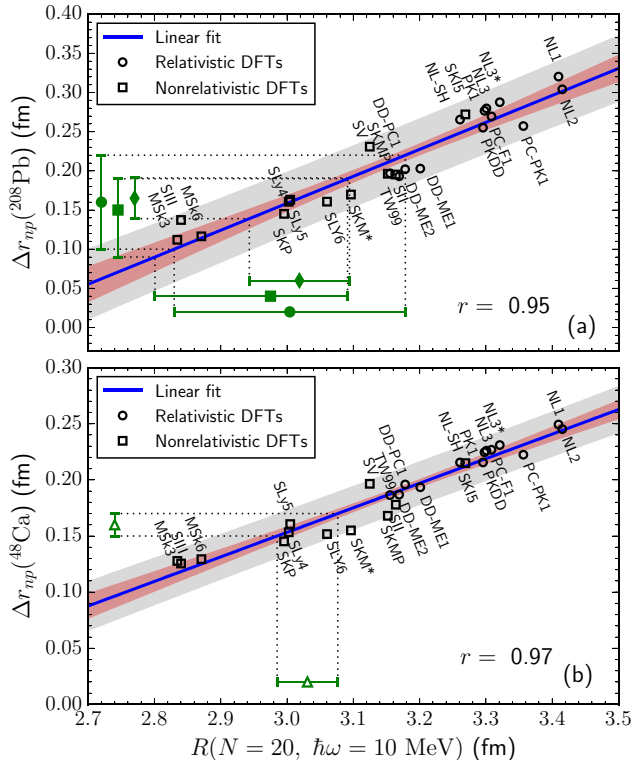


FIG. 2. (color online) Upper panel: the neutron skin thickness Δr_{np} of ^{208}Pb against the rms radius R of 20 neutrons trapped in a HO potential with $\hbar\omega = 10$ MeV for various nuclear density functionals. The inner (outer) colored regions depict the 95% confidence (prediction) intervals of the linear regression, and the Pearson's correlation coefficient r is also displayed (see, e.g., Ref. [58]). The data of Δr_{np} in different measurements with antiprotonic atoms [31] (circle), pion photoproduction [28] (square), and electric dipole polarizability [59] (diamond), are also given together with their projections on the radius of the neutron drop. Lower panel: same plot, but for the neutron skin thickness Δr_{np} of ^{48}Ca . The estimate of Δr_{np} is from a prediction of electric dipole polarizability [60].

We computed the neutron skin thicknesses Δr_{np} of ^{208}Pb and ^{48}Ca using a large sample of nuclear density functionals based on very different schemes: from non-relativistic to relativistic ones [61], from finite range meson-exchange to zero-range point-coupling ones [19]. Fig. 2 depicts Δr_{np} obtained for ^{208}Pb and ^{48}Ca as a function of the rms radius R of 20 neutrons trapped in a HO potential with $\hbar\omega = 10$ MeV. All the functionals considered here

are quite successful in describing bulk properties such as binding energies and charge radii for nuclei over the entire nuclide chart. However, one can clearly see in Fig. 2 that their predictions for Δr_{np} are very different, from 0.1 to 0.3 fm, since the isovector channels in these phenomenological functionals are loosely determined in the fitting procedures. The functionals with softer (stiffer) symmetry energy at the saturation density yield smaller (larger) Δr_{np} values [24].

A strong linear correlation is found between the neutron skin thickness Δr_{np} and the rms radius R of the 20 neutrons in the potential with $\hbar\omega = 10$ MeV. The Pearson's correlation coefficient is $r = 0.95$ (see, e.g., Ref. [58]) for ^{208}Pb and $r = 0.97$ for ^{48}Ca . We note that this strong linear correlation is universal in the realm of mean-field theory, since it is based on widely different nuclear density functionals. It reflects the fact that both the neutron skin thickness and the radius of a neutron drop are highly relevant to the behavior of the nuclear symmetry energy. Such a high quality linear correlation allows one to deduce the rms radius R from the measured Δr_{np} . In Fig. 2(a), the measured Δr_{np} of ^{208}Pb from antiprotonic atoms (circle) [31], pion photoproduction (square) [28], and electric dipole polarizability (diamond) [59] are shown. These data have their central values around 0.15 fm and agree well with each other within the errors. They determine, through the linear fit of Fig. 2(a), that the rms radius R has a central value around 3.0 fm. Note that the 16% accuracy in Δr_{np} from the electric dipole polarizability leads to a $\sim 2.5\%$ accuracy in R of the neutron drop. Apart from ^{208}Pb , the neutron skin thickness Δr_{np} of ^{48}Ca has been another recent focus of experiment, and it may provide key information for bridging DFTs and *ab initio* approaches [62]. Since the experiments for Δr_{np} of ^{48}Ca are still ongoing, an estimate of $\Delta r_{np} = 0.16 \pm 0.01$ fm from a prediction of electric dipole polarizability [60] is shown in Fig. 2(b). The resulting R for the neutron drop from the linear fit is $R = 3.04 \pm 0.04$ fm, which is consistent with the R value determined from the Δr_{np} of ^{208}Pb . Note that, in this case, the 6.25% accuracy in Δr_{np} leads to an accuracy of 1.3% in R for the neutron drop.

The linear correlations found for $N = 20$ are also obtained for neutron drops with different neutron numbers and different external traps. The only requirement inherent to this result is that the central density of the neutron drop does not differ greatly from the saturation density ($\sim 0.16 \text{ fm}^{-3}$). This condition can be readily satisfied by varying the strength of the external field; i.e., larger (smaller) neutron numbers should be associated with weaker (stronger) external fields. We have considered three different neutron drop systems, with

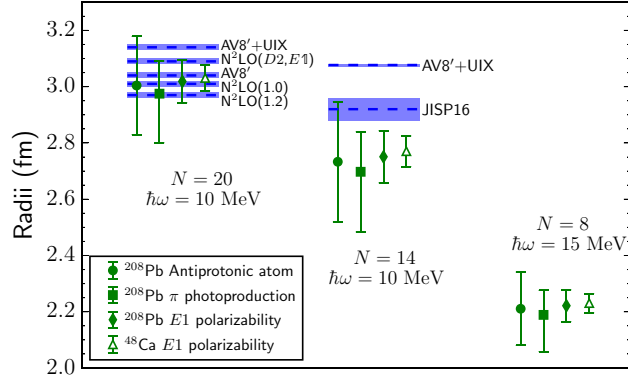


FIG. 3. (color online) The rms radii for three neutron drops determined from their linear correlations with the neutron skin thicknesses of ^{208}Pb and ^{48}Ca . For comparison, the *ab initio* results obtained using phenomenological forces and local chiral forces of Ref. [63] are also shown.

20 and 14 neutrons in a HO with $\hbar\omega = 10$ MeV, and 8 neutrons in 15 MeV. For all three systems, strong linear correlations between their rms radii and the neutron skin thickness Δr_{np} of ^{208}Pb or ^{48}Ca are found. The resulting rms radii from different data of Δr_{np} are compared in Fig. 3 with the AFDMC calculations for 20 neutrons obtained using different nuclear Hamiltonians including the Argonne AV8' and AV8'+UIX [14], and local chiral forces of Ref. [63]. We have also calculated the radial density, and verified that, in the center, the density of the drop is always within $0.16 \pm 0.02 \text{ fm}^{-3}$.

The determined radii of the $N = 14$ droplet from the skin thickness are smaller than the results with AV8'+UIX [14], showing that the UIX force might be too repulsive here. For the $N = 20$ droplet, the radii obtained from AFDMC with local chiral forces are smaller than those with AV8' and UIX forces, and they agree quite well with the radii determined by the skin thicknesses. With the development of the high-accuracy measurements of neutron skin thickness, especially the PREX and CREX programs at JLab [64], the radii of neutron drops will be measured more accurately in the near future.

Finally, we have calculated the EOS of pure neutron matter using AFDMC to fit the slope L of the symmetry energy as discussed in Refs. [37, 65]. Since the radius R of neutron drops is correlated with the skin thickness of nuclei, and the skin thickness with the value of L [40], it is interesting to plot these quantities together, see Fig. 4. The values of L for the various functionals considered are taken from Refs. [66, 67]. We find that the two quantities R and L are a bit less well correlated than R vs Δr_{np} , or Δr_{np} vs L of Ref. [40].

The Pearson's coefficient is obtained as $r = 0.92$ by fitting the density-functional results. It is interesting to note that the density-functional predictions of the correlation between R and L is compatible with *ab-initio* calculations.

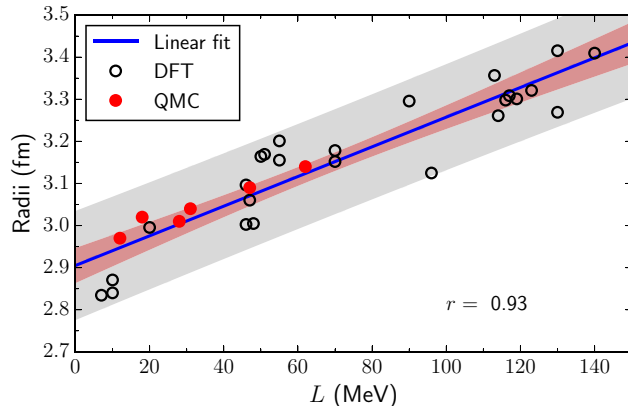


FIG. 4. (color online) The values of the slope L of the symmetry energy against rms radii of 20 neutrons in a HO with $\hbar\omega = 10$ MeV, obtained with density functional theories (open circles) and *ab initio* methods (solid circles).

In summary, the properties of neutron drops have been investigated systematically with both non-relativistic and relativistic density functional theories in comparison with results from *ab initio* calculations. The uncertainties of the realistic 3N forces and the isovector parts of density functionals are found to be large and comparable for predicting neutron drop properties. A strong linear correlation between the rms radii of neutron drops and the neutron skin thicknesses of ^{208}Pb and ^{48}Ca has been demonstrated. This correlation is universal in the realm of density functional theories, and applies to different neutron drops if their central densities do not significantly differ from saturation density. Due to its high quality, this linear correlation can be used to deduce the radii of neutron drops by measuring the neutron skin thickness, and these radii can in turn provide a useful constraint for realistic 3N forces. In view of upcoming high-precision measurements of neutron skin thicknesses in ^{208}Pb and ^{48}Ca , this correlation is likely to have an enduring impact on the understanding of multi-neutron interactions. We have also shown the correlation between radii of neutron drops with the slope of the symmetry energy. In this case, the correlation is not as strong, but the density-functional results are very close to the *ab initio* ones, suggesting that radii of confined neutrons can give important information of the slope of the symmetry energy.

Future similar calculations of radii of neutron drops in different external traps might open the way to calculate and predict L at different densities.

The authors thank Steven C. Pieper, Robert B. Wiringa, and R. V. F. Janssens for valuable discussions and careful reading of the manuscript. This work is supported by U.S. Department of Energy (DOE), Office of Science, Office of Nuclear Physics, under contract DE-AC02-06CH11357 (P.W.Z.), and by DE-AC02-05CH11231 and by the NUCLEI SciDAC project (S.G.). Computational resources have been provided by the Laboratory Computing Resource Center at Argonne National Laboratory and by Los Alamos Open Supercomputing. This research used resources of the National Energy Research Scientific Computing Center, a DOE Office of Science User Facility supported by the Office of Science of the U.S. Department of Energy under Contract No. DE-AC02-05CH11231.

-
- [1] J. Erler, N. Birge, M. Kortelainen, W. Nazarewicz, E. Olsen, A. M. Perhac, and M. Stoitsov, *Nature* **486**, 509 (2012).
 - [2] I. Tanihata, H. Hamagaki, O. Hashimoto, Y. Shida, N. Yoshikawa, K. Sugimoto, O. Yamakawa, T. Kobayashi, and N. Takahashi, *Phys. Rev. Lett.* **55**, 2676 (1985).
 - [3] Y.-Z. Qian, *Prog. Part. Nucl. Phys.* **50**, 153 (2003).
 - [4] M. Arnould, S. Goriely, and K. Takahashi, *Phys. Rep.* **450**, 97 (2007).
 - [5] D. G. Ravenhall, C. J. Pethick, and J. R. Wilson, *Phys. Rev. Lett.* **50**, 2066 (1983).
 - [6] E. F. Brown and A. Cumming, *Astrophys. J.* **698**, 1020 (2009).
 - [7] M. Buraczynski and A. Gezerlis, arXiv:1510.06417 [nucl-th].
 - [8] K. Kisamori *et al.*, *Phys. Rev. Lett.* **116**, 052501 (2016).
 - [9] S. K. Bogner, R. J. Furnstahl, H. Hergert, M. Kortelainen, P. Maris, M. Stoitsov, and J. P. Vary, *Phys. Rev. C* **84**, 044306 (2011).
 - [10] S. Gandolfi, F. Pederiva, S. Fantoni, and K. E. Schmidt, *Phys. Rev. C* **73**, 044304 (2006).
 - [11] S. Gandolfi, F. Pederiva, and S. a Beccara, *Eur. Phys. J. A* **35**, 207 (2008).
 - [12] J. Carlson, S. Gandolfi, F. Pederiva, S. C. Pieper, R. Schiavilla, K. E. Schmidt, and R. B. Wiringa, *Rev. Mod. Phys.* **87**, 1067 (2015).
 - [13] B. S. Pudliner, A. Smerzi, J. Carlson, V. R. Pandharipande, S. C. Pieper, and D. G. Ravenhall, *Phys. Rev. Lett.* **76**, 2416 (1996).

- [14] S. Gandolfi, J. Carlson, and S. C. Pieper, Phys. Rev. Lett. **106**, 012501 (2011).
- [15] P. Maris, J. P. Vary, S. Gandolfi, J. Carlson, and S. C. Pieper, Phys. Rev. C **87**, 054318 (2013).
- [16] H. Potter, S. Fischer, P. Maris, J. Vary, S. Binder, A. Calci, J. Langhammer, and R. Roth, Phys. Lett. B **739**, 445 (2014).
- [17] I. Tews, S. Gandolfi, A. Gezerlis, and A. Schwenk, Phys. Rev. C **93**, 024305 (2016).
- [18] G. A. Lalazissis, P. Ring, and D. Vretenar, eds., *Extended Density Functionals in Nuclear Structure Physics* (Springer Berlin Heidelberg, 2004).
- [19] J. Meng, ed., *Relativistic Density Functional for Nuclear Structure* (World Scientific, 2015).
- [20] S. C. Pieper, Phys. Rev. Lett. **90**, 252501 (2003).
- [21] H.-W. Hammer, A. Nogga, and A. Schwenk, Rev. Mod. Phys. **85**, 197 (2013).
- [22] P.-G. Reinhard and W. Nazarewicz, Phys. Rev. C **81**, 051303 (2010).
- [23] B. Alex Brown, Phys. Rev. Lett. **85**, 5296 (2000).
- [24] M. Centelles, X. Roca-Maza, X. Viñas, and M. Warda, Phys. Rev. Lett. **102**, 122502 (2009).
- [25] M. B. Tsang, J. R. Stone, F. Camera, P. Danielewicz, S. Gandolfi, K. Hebeler, C. J. Horowitz, J. Lee, W. G. Lynch, Z. Kohley, R. Lemmon, P. Möller, T. Murakami, S. Riordan, X. Roca-Maza, F. Sammarruca, A. W. Steiner, I. Vidaña, and S. J. Yennello, Phys. Rev. C **86**, 015803 (2012).
- [26] C. J. Horowitz, E. F. Brown, Y. Kim, W. G. Lynch, R. Michaels, A. Ono, J. Piekarewicz, M. B. Tsang, and H. H. Wolter, J. Phys. G **41**, 093001 (2014).
- [27] S. Abrahamyan *et al.* (PREX Collaboration), Phys. Rev. Lett. **108**, 112502 (2012).
- [28] C. M. Tarbert *et al.* (Crystal Ball at MAMI and A2 Collaboration), Phys. Rev. Lett. **112**, 242502 (2014).
- [29] J. Zenihiro, H. Sakaguchi, T. Murakami, M. Yosoi, Y. Yasuda, S. Terashima, Y. Iwao, H. Takeda, M. Itoh, H. P. Yoshida, and M. Uchida, Phys. Rev. C **82**, 044611 (2010).
- [30] A. Trzcíńska, J. Jastrzębski, P. Lubiński, F. J. Hartmann, R. Schmidt, T. von Egidy, and B. Kłos, Phys. Rev. Lett. **87**, 082501 (2001).
- [31] B. Kłos, A. Trzcíńska, J. Jastrzkebski, T. Czosnyka, M. Kisieliński, P. Lubiński, P. Napiorkowski, L. Pieńkowski, F. J. Hartmann, B. Ketzer, P. Ring, R. Schmidt, T. v. Egidy, R. Smolańczuk, S. Wycech, K. Gulda, W. Kurcewicz, E. Widmann, and B. A. Brown,

- Phys. Rev. C **76**, 014311 (2007).
- [32] A. Tamii *et al.*, Phys. Rev. Lett. **107**, 062502 (2011).
- [33] D. M. Rossi *et al.*, Phys. Rev. Lett. **111**, 242503 (2013).
- [34] C. J. Horowitz, S. J. Pollock, P. A. Souder, and R. Michaels, Phys. Rev. C **63**, 025501 (2001).
- [35] N. Schunck, J. Dobaczewski, J. McDonnell, W. Satua, J. Sheikh, A. Staszczak, M. Stoitsov, and P. Toivanen, Comput. Phys. Comm. **183**, 166 (2012).
- [36] T. Nikšić, N. Paar, D. Vretenar, and P. Ring, Comput. Phys. Commun. **185**, 1808 (2014).
- [37] S. Gandolfi, J. Carlson, and S. Reddy, Phys. Rev. C **85**, 032801 (2012).
- [38] A. W. Steiner and S. Gandolfi, Phys. Rev. Lett. **108**, 081102 (2012).
- [39] F. J. Fattoyev and J. Piekarewicz, Phys. Rev. C **86**, 015802 (2012).
- [40] X. Roca-Maza, M. Centelles, X. Viñas, and M. Warda, Phys. Rev. Lett. **106**, 252501 (2011).
- [41] K. E. Schmidt and S. Fantoni, Phys. Lett. B **446**, 99 (1999).
- [42] S. Gandolfi, A. Y. Illarionov, K. E. Schmidt, F. Pederiva, and S. Fantoni, Phys. Rev. C **79**, 054005 (2009).
- [43] B. S. Pudliner, V. R. Pandharipande, J. Carlson, S. C. Pieper, and R. B. Wiringa, Phys. Rev. C **56**, 1720 (1997).
- [44] A. Gezerlis, I. Tews, E. Epelbaum, S. Gandolfi, K. Hebeler, *et al.*, Phys. Rev. Lett. **111**, 032501 (2013).
- [45] A. Gezerlis, I. Tews, E. Epelbaum, M. Freunek, S. Gandolfi, K. Hebeler, A. Nogga, and A. Schwenk, Phys. Rev. C **90**, 054323 (2014).
- [46] P. Ring, Prog. Part. Nucl. Phys. **37**, 193 (1996).
- [47] Y. Tian, Z. Ma, and P. Ring, Phys. Lett. B **676**, 44 (2009).
- [48] D. Vretenar, A. V. Afanasjev, G. A. Lalazissis, and P. Ring, Phys. Rep. **409**, 101 (2005).
- [49] J. Meng, J. Peng, S. Q. Zhang, and S.-G. Zhou, Phys. Rev. C **73**, 037303 (2006).
- [50] G. A. Lalazissis, J. König, and P. Ring, Phys. Rev. C **55**, 540 (1997).
- [51] W. Long, J. Meng, N. Van Giai, and S.-G. Zhou, Phys. Rev. C **69**, 034319 (2004).
- [52] G. A. Lalazissis, T. Nikšić, D. Vretenar, and P. Ring, Phys. Rev. C **71**, 024312 (2005).
- [53] P. W. Zhao, Z. P. Li, J. M. Yao, and J. Meng, Phys. Rev. C **82**, 054319 (2010).
- [54] T. Nikšić, D. Vretenar, and P. Ring, Phys. Rev. C **78**, 034318 (2008).
- [55] S. C. Pieper, AIP Conf. Proc. **1011**, 143 (2008).
- [56] A. Sarsa, S. Fantoni, K. E. Schmidt, and F. Pederiva, Phys. Rev. C **68**, 024308 (2003).

- [57] A. Shirokov, J. Vary, A. Mazur, and T. Weber, *Phys. Lett. B* **644**, 33 (2007).
- [58] N. R. Draper and . Smith, Harry, *Applied regression analysis*, 3rd ed. (New York Wiley, 1998).
- [59] X. Roca-Maza, M. Brenna, G. Colò, M. Centelles, X. Viñas, B. K. Agrawal, N. Paar, D. Vretenar, and J. Piekarewicz, *Phys. Rev. C* **88**, 024316 (2013).
- [60] X. Roca-Maza, X. Viñas, M. Centelles, B. K. Agrawal, G. Colò, N. Paar, J. Piekarewicz, and D. Vretenar, *Phys. Rev. C* **92**, 064304 (2015).
- [61] M. Bender, P.-H. Heenen, and P.-G. Reinhard, *Rev. Mod. Phys.* **75**, 121 (2003).
- [62] G. Hagen, A. Ekstrom, C. Forssen, G. R. Jansen, W. Nazarewicz, T. Papenbrock, K. A. Wendt, S. Bacca, N. Barnea, B. Carlsson, C. Drischler, K. Hebeler, M. Hjorth-Jensen, M. Miorelli, G. Orlandini, A. Schwenk, and J. Simonis, *Nature Phys* **12**, 186 (2016).
- [63] J. E. Lynn, I. Tews, J. Carlson, S. Gandolfi, A. Gezerlis, K. E. Schmidt, and A. Schwenk, *Phys. Rev. Lett.* **116**, 062501 (2016).
- [64] <http://hallaweb.jlab.org/parity/prex>.
- [65] S. Gandolfi, J. Carlson, S. Reddy, A. W. Steiner, and R. B. Wiringa, *Eur. Phys. J. A* **50**, 10 (2014).
- [66] M. Dutra, O. Lourenço, J. S. Sá Martins, A. Delfino, J. R. Stone, and P. D. Stevenson, *Phys. Rev. C* **85**, 035201 (2012).
- [67] M. Dutra, O. Lourenço, S. S. Avancini, B. V. Carlson, A. Delfino, D. P. Menezes, C. Providência, S. Typel, and J. R. Stone, *Phys. Rev. C* **90**, 055203 (2014).